# CALCULATING THE VELOCITY OF A FAST MOVING SNOW AVALANCHE USING AN INFRASOUND ARRAY

Scott Havens*, Hans-Peter Marshall*, Jeffery B Johnson*, and Bill Nicholson†

*Center for Geophysical Investigation of the Shallow Subsurface, Boise State University, Boise, Idaho, USA
†Idaho Transportation Department, Boise, Idaho, USA

ABSTRACT: On January 19, 2012, a large D3 avalanche was recorded with an infrasound array ideally situated for observing the avalanche velocity. The avalanche crossed Highway 21 in Central Idaho during the largest avalanche cycle in the 15 years of operation and deposited approximately 8 meters of snow on the roadway. The avalanche velocity was calculated at a high spatial and temporal resolution during the 64 second event. Approximately 10 seconds prior to the main avalanche signal, a small signal originated from the direction of the start zone, which we infer to be the initial snow pack failure. The avalanche accelerated to a maximum velocity of $35.9 \pm 7.6 ms^{-1}$ within 30 seconds before impacting the highway.

KEYWORDS: Snow avalanche, infrasound, avalanche velocity, snow dynamics

## 1. INTRODUCTION

Avalanches generate acoustic signals in the 1-5 Hz bandwidth and were first detected on infrasound sensors deployed by the National Oceanic and Atmospheric Administration (NOAA) in Boulder, CO (Bedard Jr, 1989, 1994; Bedard Jr et al., 1988). The authors work led others to develop avalanche detection systems using infrasound (Chritin et al., 1996; Scott et al., 2007; Ulivieri et al., 2011).

Seismometers placed in the avalanche path can detect when an avalanche reaches each station (e.g. Vilajosana et al., 2007). The avalanche velocity can be calculated using the seismometer locations and the time when the avalanche moves over the seismometer. Vilajosana et al. (2007) found dry avalanches to move between 5 and 55 $ms^{-1}$. Kishimura and Izumi (1997) recorded avalanche velocity between 25 and 57 $ms^{-1}$ and Takeuchi et al. (2003) recorded dry and wet avalanches velocities between 20 to 43 $ms^{-1}$.

Avalanche velocity can be calculated using other techniques like video-grammetry (Vallet et al., 2004), pressure pylons placed directly in the avalanche path (Kogelnig et al., 2011), upward looking Frequency Modulated Continuous Wave (FMCW) radars (Gubler and Hiller, 1984), or FMCW doppler radar placed at the base of the path (Vriend et al., 2013). However, most of these methods are constrained to only a single avalanche path.

Corresponding author: S. Havens, Center for Geophysical Investigation of the Shallow Subsurface, Boise State University 1910 University Drive, Boise, ID 83725, USA. (scotthavens@boisestate.edu)

Here we present an avalanche event that was recorded on a nearby (less than 600 meters) infrasound array. Using array processing techniques and Monte Carlo simulations of probable source locations, we calculate the velocity and the uncertainty of the avalanche. The work has been accepted for publication in Geophysical Research Letters (Havens et al., Accepted)

## 2. 96.92 AVALANCHE EVENT

The avalanche cycle on January 19, 2012 proved to be one of the largest avalanche cycles Highway 21 has experienced in the 15 years of operational avalanche forecasting. The D3 dry avalanche occurred after 7 centimeters of water and approximately 56 centimeters of snow, two and a half days into a 7 day storm. Storm totals were 1.34 meters of snow, 0.129 meters of water, and produced 57 reported avalanches. 37 different avalanches reached the highway with between 1.5 and 8 meters of debris.

The 96.92 avalanche path produces about 2.5 avalanches per year. The avalanche path is 620 meters in length, has a vertical drop of 370 meters, and has an average slope angle of 31 degrees.

The avalanche occurred on January 19, 2012 at 16:36 UTC and lasted approximately 64 seconds. The signal amplitude (Figure 1a) shows the classic cigar shaped infrasound signal with a gradually increasing then decreasing amplitude. The amplitude changes are due to the avalanche gaining momentum and size (Kogelnig et al., 2011) before slowing to a stop on the highway.

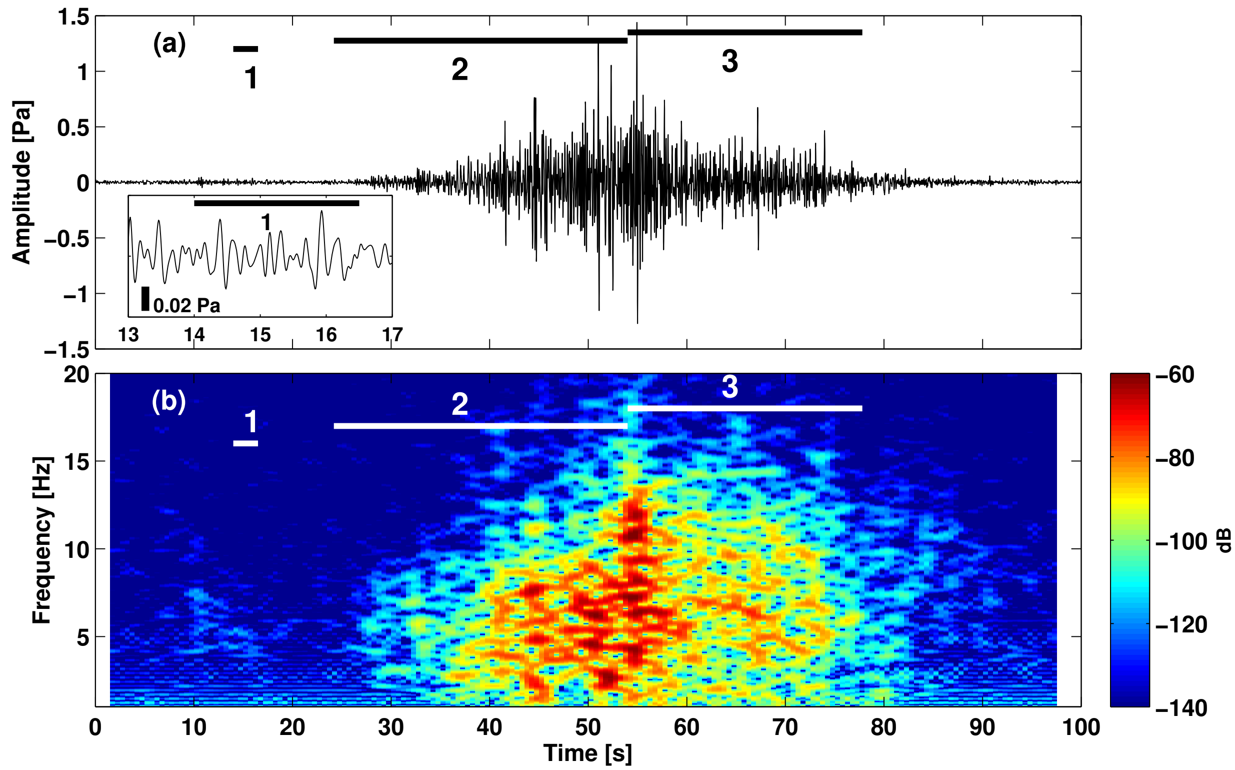


Fig. 1. (a) Avalanche signal with the three phases marked with inlay showing the whumpf signal. (b) Power spectrum of avalanche.

A small precursory signal was observed 14 seconds prior to the avalanche moving downslope (Figure 1). We hypothesize that the snowpack fracture propagation displaced the snowpack, causing a pressure wave in the air (i.e. a "whumpf", McClung and Schaerer, 2006). We believe this to be the first published example of infrasound generated from a potential snowpack failure.

## 3. METHODS

The Fisher statistic (e.g. Smart and Flinn, 1971; Blandford, 1974) measures the coherency of a signal across an array. Time shifts are applied to the signals that correspond to locations along the avalanche path. When the Fisher statistic is maximized, the time shift provides a direct estimate of the back azimuth and incidence angle to the potential source location. The time shifts were applied for a moving window of 4 seconds, overlapped by 3.5 seconds in the 1-10 Hz bandwidth.

The Fisher statistic was calculated as a function of position along the avalanche path taken from a 2 meter Digital Elevation Model (Figure 2c). The possible source location are represented by high Fisher statistic values with higher values indicating a greater probability of the avalanche location. The probable source locations were randomly sampled based on the Fisher statistic value at each time step, i.e. a higher Fisher statistic value has a higher probability of being randomly chosen. The sampled locations were smoothed to reduce large jumps before calculating the velocity. 1000 Monte Carlo simulations were performed to estimate the median and interquartile range (IQR) of the velocity.

## 4. RESULTS AND DISCUSSION

### *4.1 The Three Avalanche Phases*

The avalanche can be described in three different phases: the initial failure, acceleration in the track, and impact with the highway (Figure 2).

The first phase is a small signal with a peak amplitude of 0.035 Pa originated from the start zone 10 seconds prior to the avalanche and lasted for 2.5 seconds. We interpret the precursory signal as the fracture initiation and propagation of the snowpack. Using a string of geophones, Johnson

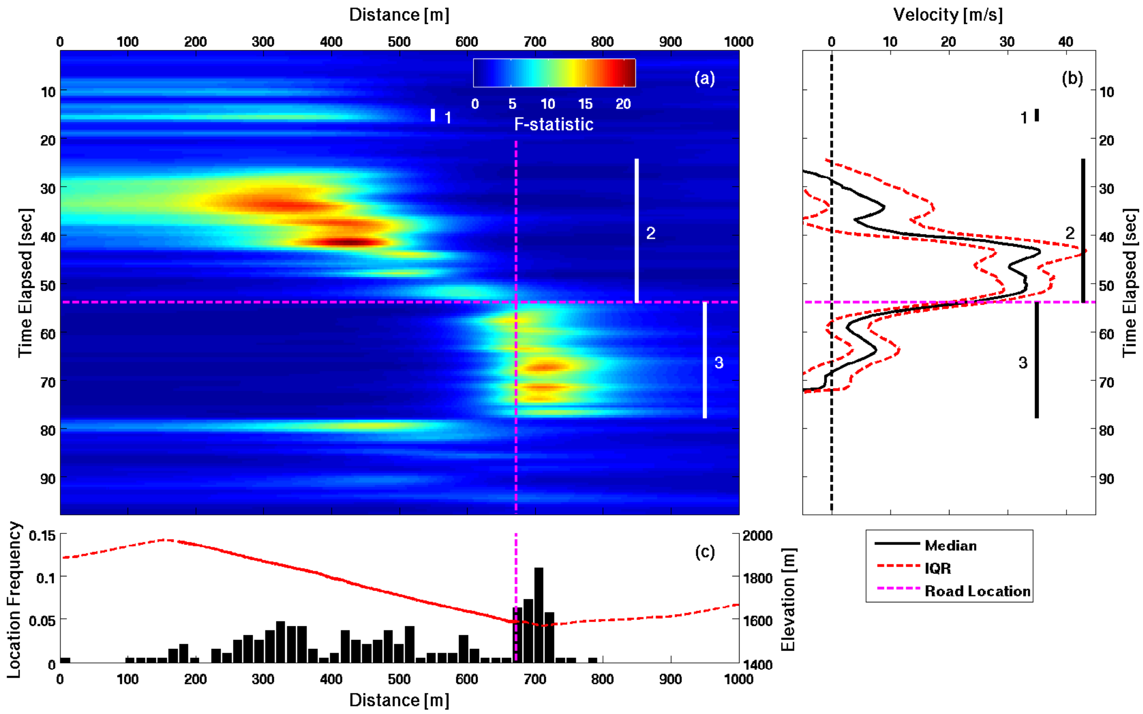


Fig. 2. (a) F-statistic evaluated at each point along the path profile. The three avalanche phases are shown with the highway location highlighted. (b) Avalanche velocity estimate. (c) 96.92 path profile in red with a histogram of the maximum F-statistic locations through time. The solid red shows the maximum extent of the 96.92 avalanche path with the snowpack failure and avalanche motion originating around 300-320 meters.

et al. (2004) measured a propagating failure away from the trigger point at a velocity of 20 $ms^{-1}$. The fracture and sudden vertical movement of the slab created a bending wave that propagated away from the trigger point. High speed video of snow stability tests have recorded fracture propagation velocities of 27 to 36 $ms^{-1}$ (van Herwijnen et al., 2010) and have estimated a 1-2 mm vertical slab displacement (Bair et al., 2012). The whumpf sound is created by the slab movement inducing a vibration in the atmosphere right above the slab (Schweizer et al., 2003). The average propagation velocity for the failure signal would be 24 $ms^{-1}$ if the fracture propagated across the entire 60 meter start zone.

The second phase starts at 24.2 seconds and lasts until 54.0 seconds when the avalanche reaches the highway (Figure 2a). The avalanche accelerates quickly to the maximum velocity of $35.9 \pm 7.6 ms^{-1}$ approximately 300 meters from the highway (43.3 seconds, Figure 2b).

The third phase occurs after 54.0 seconds when the avalanche impacts the highway and overflows into the creek for 23.8 seconds.

### *4.2 Avalanche Velocity*

The average velocity was 14.5 $ms^{-1}$ as the avalanche moved down path and was in the lower range of previous observations (e.g. Kishimura and Izumi, 1997). The velocity time series shows the characteristics of a mass gaining momentum (Figure 2b) with a small initial velocity that quickly accelerates to the maximum velocity of $35.9 \pm 7.6 ms^{-1}$ as more snow was entrained.

## 5. CONCLUSIONS

For the first time using an infrasound array, a high resolution velocity time series was calculated for an avalanche. Most studies of avalanche velocity have only calculated the average velocity (e.g. Takeuchi et al., 2003), with higher resolution estimates obtained for single paths from radar measurements (Vriend et al., 2013). With infrasound, we were able to calculate an average velocity of 14.5 $ms^{-1}$ and a maximum velocity of $35.9 \pm 7.6 ms^{-1}$.

The avalanche signal had three distinct phases. The avalanche started with the snowpack failure 10 seconds prior to the first detectable signal from the avalanche. We believe this to be the first possible weak layer failure captured on an infrasound array thanks to the close proximity of the array to the avalanche start zone. Once the avalanche gained momentum, it quickly accelerated to a maximum velocity of $35.9 \pm 7.6 ms^{-1}$ before impacting the highway. Once the avalanche reached the highway, it continued to deposit debris for 23.8 seconds before the avalanche gained momentum.

In the future, the volume and mass of snow deposited on the highway could be calculated by combining the measured infrasound signal with an avalanche dynamics models. This would prove useful for estimating highway clean-up requirements.

## ACKNOWLEDGEMENTS

The authors would like to thank the avalanche forecasters at Idaho Transportation Department for the weather and avalanche data. Support for this research was provided by Idaho Transportation Department research project RP219, NASA grant 12-EARTH12R-49 (NASA Earth and Space Sciences Fellowship), NSF EAR grant 1151662, and IRIS PASSCAL. The avalanche infrasound data can be obtained by contacting the corresponding author directly. Two anonymous reviewers provided valuable comments that improved this manuscript.

## REFERENCES

Bair, E. H., R. Simenhois, K. Birkeland, and J. Dozier, 2012: A field study on failure of storm snow slab avalanches. *COLD REGIONS SCIENCE AND TECHNOLOGY*, **79-80**, 20–28, doi:{10.1016/j.coldregions.2012.02.007}.

Bedard Jr, A. J., 1989: Detection of avalanches using atmospheric infrasound. *Proceedings ofWestern Snow Conference, Fort Collins, CO*.

Bedard Jr, A. J., 1994: An evaluation of atmospheric infrasound for monitoring avalanche. *Proceedings of 7th International Symposium on Acoustic Sensing and Associated Techniques of the Atmosphere and Oceans, Boulder, CO*.

Bedard Jr, A. J., G. E. Greene, J. Intrieri, and R. Rodriguez, 1988: On the feasibility and value of detecting and characterizing avalanches remotely by monitoring radiated sub-audible atmospheric sound at long distances. *Proceedings of A Multidisciplinary Approach to Snow Engineering, Santa Barbara, CA*.

Blandford, R. R., 1974: An automatic event detector at the tonto forest seismic observatory. *Geophysics*, **39 (5)**, 633–643.

Chritin, V., M. Rossi, and R. Bolognesi, 1996: Acoustic detection system for operational avalanche forecasting. *Proceedings of the 1996 International Snow Science Workshop, Banff, Canada*.

Gubler, H., and M. Hiller, 1984: The use of microwave FMCW radar in snow and avalanche research. **9**, 109–119.

Havens, S., H.-P. Marshall, J. B. Johnson, and B. Nicholson, Accepted: Calculating the velocity of a fast moving snow avalanche using an infrasound array. *Geophysical Research Letters*.

Johnson, B., J. Jamieson, and R. Stewart, 2004: Seismic measurement of fracture speed in a weak snowpack layer. *COLD REGIONS SCIENCE AND TECHNOLOGY*, **40 (1-2)**, 41–45, doi:{10.1016/j.coldregions.2004.05.003}.

Kishimura, K., and K. Izumi, 1997: Seismic signals induced by snow avalanche flow. *NATURAL HAZARDS*, **15 (1)**, 89–100, doi:{10.1023/A:1007934815584}.

Kogelnig, A., E. Surinach, I. Vilajosana, J. Huebl, B. Sovilla, M. Hiller, and F. Dufour, 2011: On the complementariness of infrasound and seismic sensors for monitoring snow avalanches. *NATURAL HAZARDS AND EARTH SYSTEM SCIENCES*, **11 (8)**, 2355–2370, doi:{10.5194/nhess-11-2355-2011}.

McClung, D. M., and P. Schaerer, 2006: *The Avalanche Handbook*. The Mountaineers, Seattle, WA.

Schweizer, J., J. Jamieson, and M. Schneebeli, 2003: Snow avalanche formation. *REVIEWS OF GEOPHYSICS*, **41 (4)**, doi:{10.1029/2002RG000123}.

Scott, E. D., C. T. Hayward, R. F. Kubichek, J. C. Hamann, J. W. Pierre, B. Comey, and T. Mendenhall, 2007: Single and multiple sensor identification of avalanche-generated infrasound. *COLD REGIONS SCIENCE AND TECHNOLOGY*, **47 (1-2)**, 159–170, doi:{10.1016/j.coldregions.2006.08.005}, International Snow Science Workshop, Jackson Hole, WY, SEP 19-24, 2004.

Smart, E., and E. A. Flinn, 1971: Fast frequency-wavenumber analysis and fisher signal detection in real-time infrasonic array data processing. *Geophysical Journal International*, **26 (1-4)**, 279–284, doi: 10.1111/j.1365-246X.1971.tb03401.x, URL http://gji.oxfordjournals.org/content/26/1-4/279.abstract, http://gji.oxfordjournals.org/content/26/1-4/279.full.pdf+html.

Takeuchi, Y., K. Yamanoi, Y. Endo, S. Murakami, and K. Izumi, 2003: Velocities for the dry and wet snow avalanches at Makunosawa valley in Myoko, Japan. *COLD REGIONS SCIENCE AND TECHNOLOGY*, **37 (3)**, 483–486, doi:{10.1016/S0165-232X(03)00086-7}, International Snow Science Workshop, PENTICTON, CANADA, SEP 29-OCT 04, 2002.

Ulivieri, G., E. Marchetti, M. Ripepe, I. Chiambretti, G. De Rosa, and V. Segor, 2011: Monitoring snow avalanches in Northwestern Italian Alps using an infrasound array. *COLD REGIONS SCIENCE AND TECHNOLOGY*, **69 (2-3, SI)**, 177–183, doi:{10.1016/j.coldregions.2011.09.006}.

Vallet, J., B. Turnbull, S. Joly, and F. Dufour, 2004: Observations on powder snow avalanches using videogrammetry. *COLD REGIONS SCIENCE AND TECHNOLOGY*, **39 (2-3)**, 153–159, doi:{10.1016/j.coldregions.2004.05.004}, Snow and Avalanches Conference, Nice, FRANCE, APR, 2003.

van Herwijnen, A., J. Schweizer, and J. Heierli, 2010: Measurement of the deformation field associated with fracture propagation in weak snowpack layers. *JOURNAL OF GEOPHYSICAL RESEARCH-EARTH SUR-*

*FACE*, **115**, doi:{10.1029/2009JF001515}.

Vilajosana, I., G. Khazaradze, E. Surinach, E. Lied, and K. Kristensen, 2007: Snow avalanche speed determination using seismic methods. *COLD REGIONS SCIENCE AND TECHNOLOGY*, **49 (1)**, 2–10, doi:{10.1016/j.coldregions.2006.09.007}, General Assembly of the European-Union-of-Geosciences, Vienna, AUSTRIA, APR 24-29, 2005.

Vriend, N. M., J. N. McElwaine, B. Sovilla, C. J. Keylock, M. Ash, and P. V. Brennan, 2013: High-resolution radar measurements of snow avalanches. *GEOPHYSICAL RESEARCH LETTERS*, **40 (4)**, 727–731, doi:{10.1002/grl.50134}.